Blood cultures at baseline and during persistent candidemia contain populations of genetically diverse *Candida albicans* strains that may differ in echinocandin tolerance and virulence

Giuseppe Fleres,[1] Shaoji Cheng,[1] Hassan Badrane,[1] Christopher L. Dupont,[2] Josh L. Espinoza,[2] Darren Abbey,[3] Eileen Driscoll,[1] Anthony Newbrough,[1] Binghua Hao,[1] Akila Mansour,[4] *M. Hong Nguyen,[1,4 #] *Cornelius J. Clancy[1,5]

[1]University of Pittsburgh, Pittsburgh, PA, USA
[2]J. Craig Venter Institute, La Jolla, CA, USA
[3]University of Minnesota, Minneapolis, MN, USA
[4]University of Pittsburgh Medical Center, Pittsburgh, PA, USA
[5]VA Pittsburgh Healthcare System, Pittsburgh, PA, USA

*These authors contributed equally: M. Hong Nguyen, Cornelius J. Clancy. The order in which they are listed is based on mutual consent

Running title: Diverse *C. albicans* populations in patients with candidemia

[#]Corresponding author:
M. Hong Nguyen, M.D.
University of Pittsburgh
Biomedical Science Tower, Starzl Institute
200 Lothrop Street, E-1052
Pittsburgh, PA 15203
Email: MHN5@pitt.edu
Phone: 412-383-5193

Abstract: 250 words

Text: 4930 words

Abstract.

It is unknown whether within-patient *Candida albicans* diversity is common during bloodstream infections (BSIs). We determined whole genome sequences of 10 *C. albicans* strains from blood cultures (BCs) at baseline (*n*=4 patients) and during persistent BSIs (3 of 4 patients). BCs contained mixed populations of strains that differed by single nucleotide polymorphisms (*n*=4 patients), chromosome (Chr) 5 or 7 aneuploidy (*n*=2), and loss of heterozygosity (*n*=1). Chr7 trisomy (Tri7) strains from patient MN were attenuated for hyphal and biofilm formation *in vitro* compared to euploid strains, due to *NRG1* over-expression. However, Tri7 strain M1 underwent filamentation during disseminated candidiasis (DC) in mice. M1 was more fit than euploid strain M2 during DC and gastrointestinal colonization/infection, and in blood *ex vivo*. M1 and M2 exhibited identical echinocandin minimum inhibitory concentrations, but M2 was more tolerant to micafungin *in vitro*. Furthermore, M2 was more competitive with M1 in mouse kidneys following micafungin treatment than it was in absence of micafungin. Tri7 strains represented 74% of patient MN's baseline BC population, but after 1d and 3d of echinocandin treatment, euploid strains were 93% and 98% of the population, respectively. Findings suggest that echinocandin tolerant, euploid strains were a subpopulation to more virulent Tri7 strains at baseline and then selected upon echinocandin exposure. In conclusion, BCs in at least some patients are comprised of diverse *C. albicans* populations not recognized by the clinical lab, rather than single, genetically and phenotypically identical strains. Clinical relevance of *C. albicans* diversity and antifungal tolerance merits further investigation.

Keywords: *Candida albicans*; Bloodstream infections; Genomic diversity; Echinocandin tolerance; Aneuploidy; Chromosome 7 trisomy

Introduction.

The yeast *Candida albicans* is a commensal organism of the human gastrointestinal (GI) tract and other mucosal surfaces, which can cause invasive infections of the bloodstream and deep tissues in settings of disturbed homeostasis. *C. albicans* bloodstream infections (BSIs) are associated with mortality rates of 20%-40%. *C. albicans* strains from fecal and oral samples from healthy volunteers demonstrate witsupplhin-host genetic and phenotypic diversity.[1,2] Whole genome sequences (WGSs) of longitudinal *C. albicans* strains from humans or infected mice often reveal substantial genome plasticity,[3-6] which likely facilitates adaptation to disparate environmental conditions.[4,5,7]

The long-standing paradigm is that most fungal or bacterial BSIs, including candidemia, reflect proliferation of a single, genetically identical strain that passes through a bottleneck ("single organism" hypothesis).[8-10] To date, only 3 papers have assessed bacterial or fungal genomic diversity during BSIs by WGSing strains from multiple colonies from blood cultures (BCs) of individual patients. In the first study, genetic variant strains of the same clonal group were identified in 36% of patients with *Staphylococcus aureus* bacteremia.[11] Phenotypes of strains were not assessed. We recently published the other 2 studies, demonstrating within-patient genetic and phenotypic diversity among *Candida glabrata* and carbapenem-resistant *Klebsiella pneumoniae* (CRKP) strains from BCs of patients with BSIs.[12,13] We identified mixed populations of antimicrobial-resistant and susceptible strains within single BC bottles from the time of BSI diagnosis, which were not recognized by the clinical laboratory. Within-patient *C. glabrata* strains differed by single nucleotide polymorphisms (SNPs) and, to a lesser extent, insertions-deletions (indels), gene copy number variations (CNVs), chromosomal rearrangements and presence/absence of specific genes. These data challenge the single organism hypothesis, and suggest a new, population-based paradigm for BSIs by commensal microbes.

C. albicans is the most intrinsically virulent *Candida* sp. and the leading cause of candidemia. *C. albicans* differs from *C. glabrata* in having a diploid, rather than haploid genome. It is unclear if *C. albicans* strains from positive BCs exhibit genetic and phenotypic diversity like *C. glabrata* strains. Our primary objective in this study was to determine whether contemporaneous *C. albicans* strains from positive BCs of individual patients with BSIs were genetically and phenotypically distinct. In our previous studies, we only characterized *C. glabrata* and CRKP from baseline BCs. A second objective here was to compare diversity of *C. albicans* strains from longitudinal BCs of individual patients with persistent BSIs.

Results.

WGSs of *C. albicans* strains. Clinical characteristics of 4 patients with *C. albicans* BSIs are summarized in Table 1. Of note, none of the patients had a history of candidiasis or receipt of antifungal agents within the preceding 90 days (90d). *C. albicans* index strains (i.e., those recovered by the clinical lab) were susceptible to azoles, echinocandins and amphotericin B. Patients were initially treated with an echinocandin, and later received fluconazole; 1 patient (MN) also received amphotericin B. BSI persisted after the initiation of antifungal treatment in 3 patients (AB, MN, QR).

We streaked 10 µL from positive BCs onto Sabouraud Dextrose Agar (SDA) plates, which were incubated at 35°C for 48 hours (h). Within each patient, colonies were morphologically indistinguishable. For patient G, we recovered the index strain (labeled as G1) and a strain from each of 9 randomly selected colonies (G2-G10) from the baseline (d0) BC. For the other 3 patients, we studied 5 strains each at baseline and from the last positive BCs (collected 3d (patient AB), 12d (QR) and 13d (MN) after baseline) [Table 1]. The 40 strains (10 from each patient) underwent Illumina Next-Seq WGSing. Assembly details are presented in Supplemental File 1. Strains had 8 pairs of chromosomes and 14.24-14.82 Mbp genomes. On

average, 98% of reads were aligned to reference *C. albicans* SC5314 genome (range: 96%-99%).

Genetic diversity of *C. albicans* strains. We generated a high-resolution phylogenetic tree for the 40 strains based on core genome SNPs [Figure 1]. Strains clustered by patient and segregated into 3 clades: 1) patient AB, 2) patient MN, 3) patients QR and G. SNP distance matrices are shown in Supplemental File 2.

Within individual patients, strains differed by the following numbers of core genome SNPs (defined as SNPs present in ≥ 1 strain but not all 10 strains from a given patient): 0 to 7 (AB), 7 to 42 (G), 3 to 36 (MN) and 8 to 28 (QR) [Table 2]. Within 3 patients, strains also differed by the following numbers of indels: 1 to 8 (G), 0 to 9 (MN), and 1 to 6 (QR) [Table 2; Supplemental File 3]. The most striking within-patient differences among strains were large-scale genetic variations that were observed in 3 of 4 patients (G, MN, QR) [Figure 2A-C; Supplemental Figure 1; Supplemental File 4]. Within 2 patients (G and MN), strains differed by whole chromosome aneuploidies. In patient G, strain G1 exhibited trisomy of chromosome (Chr) 5 (Tri5); other strains were euploid for Chr5 [Figure 2A]. In patient MN, 4 of 5 strains from the baseline BC (M1, M3, M4, M5) exhibited trisomy of Chr7 (Tri7); 1 of 5 strains from baseline (M2) and all 5 strains from d13 (N1-N5) were euploid for Chr7 [Figure 2B]. Ploidy was confirmed for G and MN strains by quantitative real-time PCR (qPCR) [Supplemental Figure 2].[12,14] In patient QR, loss of heterozygosity (LOH) encompassing ~300 Kbp at the end of the left arm of Chr1 was detected in 7 of 10 strains, including 2 of 5 baseline (Q1, Q2) and all 5 d12 (R1-R5) strains [Figure 2C]. Strains R1-R5 also had segmental LOH encompassing ~4.5 Kbp immediately preceding the first major repeat sequence on the left arm of Chr7, which was not present in baseline strains Q1-Q5. The only differences in SNP density among QR strains were in regions of LOH. Within-patient AB strains did not show large-scale genetic variations [Supplemental Figure 1].

Screening phenotypes of *C. albicans* strains. Since yeast-hyphal morphogenesis is an established virulence trait in *C. albicans*, we tested the strains for hyphal formation in liquid and on solid media. Strains from patients AB and QR formed normal hyphae in liquid media (YPD with 10% fetal bovine serum, RPMI1640 with 2% glucose, Spider; 37°C) and on solid agar (RPMI1640 with 2% glucose, Spider, M199; 30°C). Strains from patient MN formed normal hyphae in liquid media. On solid agar, however, all 4 Tri7 strains (baseline strains M1, M3, M4, M5) were impaired in hyphal formation, whereas all 6 euploid strains (baseline M2 and d13 N1-N5) formed robust hyphae [Figure 3]. Strains from patient G were impaired in hyphal formation in liquid media and on solid agar [Supplemental Figure 3].

Next, we tested strains for antifungal susceptibility. All were susceptible to echinocandins and azoles (within-patient minimum inhibitory concentrations (MICs) within 2-fold) [Supplemental Table 1].

Phenotypic diversity of *C. albicans* strains from patient MN. We focused on strains from patient MN because they demonstrated clear genetic differences, and Tri7 and euploid strains exhibited distinct phenotypes. In addition, serial positive BCs collected over 13d were available for study. The timeline of *C. albicans*-positive BCs and antifungal treatment for patient MN is shown in Figure 4.

We first tested MN strains for susceptibility to cell wall-active and other stress-inducing agents. The *C. albicans* cell wall is a barrier to host immune responses and environmental stressors, and cell wall integrity is critical for survival within the host and pathogenicity. We spotted serial ten-fold dilutions of each MN strain onto SDA plates impregnated with specific agents. Tri7 strains (M1, M3, M4, M5) were more susceptible to Congo red (200 µg/mL), sodium dodecyl sulfate (0.04%) and micafungin (0.03 µg/mL) at 39ºC and 30ºC than were euploid strains [Figure 5]. There were no significant differences among strains in presence of

fluconazole (1 µg/mL), methyl methane sulfonate (0.02%), hydrogen peroxide (H_2O_2, 2.5mM), sodium chloride (1M) or caffeine (10 mg/mL).

BSI in patient MN persisted despite echinocandin therapy, but echinocandin MICs of serial strains did not change. Therefore, we evaluated Tri7 and euploid MN strains for tolerance to micafungin (defined as enhanced growth of some strains compared to others in presence of drug, without changes in MIC) using disk diffusion and liquid microdilution tolerance assays.[15,16] In the former, we measured fraction of growth (FoG) within the zone of inhibition relative to maximum possible growth.[15,16] Mean FoG_{80}, FoG_{50} and FoG_{20} (FoG within zone of 80%, 50% and 20% inhibition) of euploid strains were higher than those of Tri7 strains (p=0.05, 0.03 and 0.008, respectively) [Figure 6]. In microdilution assays, we quantified supra-MIC growth (SMG, defined as average growth within micafungin-containing wells above MIC_{50}/growth in absence of micafungin). Mean SMG of euploid strains was higher than that of Tri7 strains (p=0.0003) [Figure 6]. Taken together, FoG and SMG data demonstrated that euploid strains were more tolerant than Tri7 strains to micafungin.

We then tested MN strains for biofilm production using a crystal violet assay. Biofilm formation enables *C. albicans* to adhere to tissues or other surfaces, form complex communities, reduce susceptibility to antifungal agents and host immune responses, and establish persistent infections. We showed that Tri7 strains produced <30% of the biofilm that was generated by euploid strains [Figure 7; p-values< 0.0001].

Decreased filamentation of some *C. albicans* strains with Tri7 has been linked to dose-dependent expression of Chr7 gene *NRG1*, which encodes a negative regulator of certain hyphal genes.[14] We hypothesized that defects in hyphal and biofilm formation in Tri7 strains from patient MN were linked to *NRG1* over-expression. We first demonstrated by qRT-PCR that *NRG1* expression by Tri7 strain M1 was ~1.5 fold higher than that by euploid strains [Supplemental Figure 4A]. [17] We next created *NRG1* over-expression strains in euploid M2 and

N1 backgrounds (referred to as strains M2-Nrg1OE and N1-Nrg1OE, respectively). *NRG1* expression by M2-Nrg1OE and N1-Nrg1OE was ~1.8-fold and ~1.6-fold higher than by the respective euploid parent strains (p=0.001) [Supplemental Figure 4A]. As hypothesized, *NRG1* over-expression strains had reduced hyphal and biofilm formation compared to euploid parent strains (p-values <0.0001) Supplemental Figures 4B-C].

Competitive fitness and virulence of MN strains. Since Tri7 and euploid strains comprised a mixed population within patient MN's baseline BC, we studied competitive fitness of M1 and M2 under various conditions using bar-coded strains. Bar-coded Tri7 M1 and euploid M2 strains did not differ from respective M1 and M2 parent strains during growth in YPD media, by echinocandin MICs or in hyphal formation on solid agar.

Competitive growth *in vitro* and in blood *ex vivo*. We conducted competitive growth assays for bar-coded M1 and M2 (1:1 inoculum ratio, $1x10^4$ colony forming units (CFUs)/mL each) in liquid YPD media at 39°C in presence or absence of H_2O_2 (1 mM) or micafungin (0.125 µg/mL).[14] There were no significant differences in competitive fitness between strains over 3, 6 or 9d in YPD alone or in presence of H_2O_2, as determined by bar code sequencing [Figure 8A]. Strain M2 was more fit than M1 at each time point in the presence of micafungin (p <0.0001), consistent with FoG and SMG tolerance data above.

During *ex vivo* competitive assays in fresh blood from a healthy volunteer at 37°C, bar-coded Tri7 M1 was significantly more fit than bar-coded euploid M2 over 1, 3 and 7d (1:1 inoculum ratio, $1x10^4$ CFUs)/mL each) [Figure 8B].

Competitive mouse model of GI colonization.[14] We co-infected male and female mice with bar-coded M1 and M2 (1:1 ratio, $1x10^8$ CFUs each) by gavage. M1 significantly out-competed M2 within stool on d1, d3 and d7 [Figure 8C], and in ileum and colon on d7 [Figure 8D].

Competitive mouse model of disseminated candidiasis (DC). We co-infected mice via lateral tail vein with bar-coded M1 and M2 (1:1 ratio, $5x10^5$ CFUs each). Tri7 M1 significantly out-competed euploid M2 within kidneys, the major target organ during DC, at d1, 3 and 7 [Figure 8E]. We also treated a group of M1:M2 co-infected mice with a single dose of micafungin (8.3 mg/kg/mouse intraperitoneal, 30 minutes post-infection). Strain M2 was 59% more competitive with M1 in kidneys at 24h following treatment than it was in absence of micafungin [Figure 8D].

Mouse model of mono-infection DC. Finally, we performed single strain infections in which mice were inoculated intravenously with either bar-coded M1 or M2 ($1x10^6$ CFU). Tri7 M1 burdens were significantly higher than euploid M2 burdens within kidneys at d1 and 3 [Supplemental Figure 5]. Both M1 and M2 were present as mixtures of yeast and filamentous morphologies within kidneys [Figure 9].

Tri7 strains in longitudinal and spiked BCs. We collected serial positive BC bottles from patient MN over 13d [Figure 4]. Antifungal treatment was initiated with an echinocandin on d2. To estimate point prevalence of strains differing in Chr7 ploidy, we screened 96 strains from each BC for attenuated biofilm formation. Strains with biofilm formation that was < 30% of that formed by euploid strain M2 were classified as Tri7; results were confirmed by qPCR of ≥ 10 strains from baseline and d13 BCs [Supplemental Table 2; Supplemental File 5]. Percentages of Tri7 strains were 74% (baseline, 71/96), 7% (d3, 7/96), 2% (d5, 2/96), 2% (d10, 2/96) and 0% (d13, 0/96).

To assess Tri7 stability, we spiked strain M1 into a sterile BC bottle and incubated at 37ºC until turbidity was evident (between 24 to 48h). Aliquots were sub-cultured on SDA plates at 30ºC for 48h, and each of 10 strains from randomly selected colonies was shown to still harbor Tri7 by WGS [Supplemental Figure 6].

Discussion.

We demonstrated, for the first time, that *C. albicans* strains from positive BCs of individual patients were genetically and phenotypically diverse. The most striking within-patient genetic differences among strains were whole chromosome aneuploidies and LOH, which were identified in 3 of 4 patients. In patient MN, Tri7 and euploid strains were equally fit during growth in liquid media, and they exhibited similar susceptibility to echinocandins, as measured by MICs. Euploid strains, however, were more tolerant to the echinocandin micafungin than Tri7 strains by disk diffusion (FoG), liquid microdilution (SMG) and competitive growth assays. In contrast, representative Tri7 strain M1 was more fit than euploid strain M2 during growth in human blood *ex vivo*, and during mouse models of GI colonization and DC. M2 was significantly more competitive with M1 in mouse kidneys following micafungin treatment of DC than it was in the absence of micafungin. Along these lines, Tri7 strains predominated in patient MN's baseline BC (74% of the population), but they were largely replaced by euploid strains after 1 and 3d of echinocandin treatment (93% and 98% euploid, respectively). By d13 of BSI, 100% of BC strains were euploid. Taken together, the data suggest that Tri7 strains were more intrinsically virulent than euploid strains, which conferred an advantage at baseline in absence of antifungal exposure. Echinocandin tolerant, euploid strains that were present at baseline but unrecognized by the clinical lab emerged as dominant within patient MN's bloodstream upon echinocandin exposure. We conclude that positive BCs in at least some patients are comprised of diverse *C. albicans* populations rather than single, genetically identical strains. In certain patients, strains with tolerance or other attenuated responses to antifungals may be selected from a pre-existing subpopulation, rather than arising *de novo*.

Results from this study and our previous findings that *C. glabrata*- and CRKP-positive BCs also contain genetically and phenotypically diverse strains challenge the single organism

hypothesis of BSI pathogenesis.[12,13] Our *C. albicans* data are plausible. Large-scale genome variants like aneuploidy and LOH are commonly encountered during *C. albicans* microevolution *in vitro*, in response to antifungals and in mouse models of candidiasis.[5,14,18-21] Aneuploidy can involve any of *C. albicans*' chromosomes, with positive or negative consequences for fitness and antifungal resistance depending on specific chromosome involvement, strain background and environmental conditions.[22-24] Tri7 has been observed in *C. albicans* clinical strains and in strains of diverse genetic backgrounds during GI colonization of mice.[5,14,21] Our findings that a Tri7 strain was attenuated for hyphal formation *in vitro* compared to a euploid partner strain, while exhibiting enhanced GI colonization, invasion of ileum and colon, and hematogenous infection of kidneys in mice were consistent with data for some previously studied Tri7 strains.[14,21,24] Finally, in a recent multicenter study, 8.1% of *Candida*-positive clinical cultures exhibited heterogenous echinocandin or azole susceptibility when 5 strains from independent colonies were tested.[25] Our studies of *C. albicans*, *C. glabrata* and CRKP BSIs suggest that clinical and microbiology lab practices should consider microbial populations, rather than focusing solely on single, putatively causative strains.

Our *C. glabrata* study is the only other investigation of within-patient diversity among *Candida* strains during BSIs. While genetic and phenotypic diversity, including differences in virulence, was observed among strains of both spp. in individual BCs, other findings of the studies were unique. The predominant within-patient genetic differences among *C. glabrata* strains from baseline BCs of 10 patients were core genome SNPs and indels.[12] Within-patient SNPs and indels were less prevalent among *C. albicans* strains from BCs of 4 patients. In contrast, aneuploidies were identified among *C. albicans* populations, but not among *C. glabrata*. In 2 patients, *C. glabrata* populations in baseline BCs were a mixture of antifungal-susceptible and resistant strains. In 1 of these patients, fluconazole-resistant, SCV *C. glabrata* that was unrecognized in the baseline BC was recovered from a treatment failure BC. In the

other patient, unrecognized fluconazole-resistant, *PDR1* mutant *C. glabrata* at baseline was identified in a treatment failure BC. We did not identify antifungal-resistant *C. albicans* in BCs, even though 3 of 4 patients had persistent BSI for median of 12d. In part, discrepancies in antifungal resistance findings between studies may stem from differences in patients' histories. None of the patients with *C. albicans* BSI had prior antifungal exposure or invasive candidiasis, whereas 50% and 40% of patients with *C. glabrata* BSI were heavily azole-experienced or had previous candidiasis, respectively. Future studies will elaborate whether differences between spp. in our papers have biologic explanations. Haploid organisms like *C. glabrata* adapt faster than diploid organisms, such as *C. albicans*, especially under stress.[26] In the setting of antifungal pressure, SNPs are a mechanism by which *C. glabrata* may rapidly adapt. *C. glabrata* also has unique capacity to survive and proliferate within macrophages, which represent a reservoir from which stress-tolerant and/or antifungal-resistant mutants emerge.[27]

In most cases of failed treatment of candidemia, an antifungal resistant strain, as defined by MIC, is not identified.[28] Echinocandin tolerance has been described for *C. albicans* strains *in vitro* but its clinical significance is unclear.[29,30] Tolerance to fluconazole, a fungistatic drug, has been reported in some patients failing fluconazole treatment of *C. albicans* BSIs, although its broad clinical relevance is not validated.[15] Echinocandin tolerance of *C. albicans* has been linked to Chr2 and Chr5 aneuploidies likely to impact cell wall regulation, but has not been associated with Tri7.[29-33] Likewise, the clinical relevance of *Candida* strain diversity in virulence is not established. While hyphal and biofilm formation are considered classic *C. albicans* virulence determinants, it is more precise to understand bidirectional regulation of yeast-hyphal morphogenesis and biofilm maturation, as dictated by the local environment, as crucial to commensalism and pathogenesis.[34] It is well recognized that certain *C. albicans* strains, like Tri7 strains here, may manifest defects in filamentation on solid agar, but not in liquid media *in vitro* or within target organs *in vivo*. Moreover, strains with attenuated virulence attributes *in vitro*

such as impaired filamentation or biofilm formation (as also exhibited by Tri7 strains) may manifest full or even heightened pathogenic capacity *in vivo*. In the end, *C. albicans* is an opportunistic pathogen that does not depend upon a dominant virulence factor, but rather a complex interplay of numerous properties that optimize survival in various *in vivo* niches. At least in part, attenuated hyphal formation by Tri7 strains *in vitro* has been attributed here and elsewhere to gene dosage over-expression of *NRG1*, which was initially described as a transcriptional repressor of hyphal and certain stress response genes in *C. albicans* SC5314.[14] It is now apparent that *NRG1* exerts variable effects on gene expression, filamentation, fitness and virulence depending on strain background.[14,35,36] Tri7 was not linked to aberrant *C. albicans* biofilm formation or echinocandin responsiveness prior to this study, although high levels of *NRG1* expression were shown to limit biofilm maturation and lead to increasing dispersion of yeast cells from immature biofilm.[37] Further research is needed into the potential contributions of antifungal tolerance and, more broadly, *Candida* genetic and phenotypic diversity to outcomes of human infections.

Tri7 was stable in strain M1 following incubation in spiked BC bottles, suggesting that euploid strains emerged during persistent BSI of patient MN rather than *ex vivo*. This finding was notable since changes in ploidy by *C. albicans* are often reversible adaptations to stress. We propose that most of the strain diversity we observed in BCs was likely to have arisen during GI commensalism (or at some other site of colonization), as a large *C. albicans* population engaged in long-term interaction with the host.[6] We recognize that we may have failed to identify important genetic or phenotypic variants by studying only 10 *C. albicans* strains per patient. It is feasible that genetic variants other than differences in Chr7 ploidy also contribute to important phenotypes. For example, strains with Chr1 LOH seemed to emerge in persistent BCs from patient QR. LOH, like aneuploidy, is a common *C. albicans* adaptation to antifungals and other stresses. The significance of LOH in QR strains is worthy of future

investigation. We acknowledge that results here or from our *C. glabrata* BSI study cannot necessarily to extrapolated to other *Candida* spp., other opportunistic commensal microbes, or other sites of infection. Along these lines, the extent and type of diversity we describe may reflect features that are particular to our cases. Indeed, patients were severely ill and had complex medical and surgical histories.

In conclusion, we demonstrated that positive BCs from individual patients with BSIs contained mixed populations of *C. albicans* strains that differed by combinations of aneuploidies, LOH and SNPs, and in echinocandin tolerance and virulence attributes. Studies to assess the clinical relevance of *Candida* diversity are indicated, as is research into understanding how diversity and adaptation of various microbes facilitates commensalism and disease. If results here and from our studies of *C. glabrata* and CRKP BSIs are validated, clinical and microbiology lab practices may need to be revised to consider microbial populations.

Materials and Methods.

Ethics statement. This study was approved by the University of Pittsburgh Institutional Review Board through an Expedited Review according to the OHRP, 45 CFR 46.110 and FDA 21 CFR 56.110. Mouse experiments were approved by the University of Pittsburgh Animal Care and Use Committee.

Reagents, primers and plasmids are listed in Supplemental Tables 3, 4 and 5, respectively.

Clinical strains and growth conditions.[12] BC bottles from patients with *C. albicans* BSI were obtained from the UPMC clinical microbiology laboratory, as were strains used by the clinical lab for species identification and susceptibility testing (index strains). We streaked 10 µL from positive BC bottles onto 2 SDA plates and incubated for 48h at 35°C. A strain isolated from each of 4–9 morphologically indistinguishable colonies and the index strains from each BC underwent Illumina NextSeq WGSing. Strains are listed in Supplemental Table 5.

Illumina short-read sequencing and bioinformatic analysis. DNA extraction, library preparation and genome analysis were performed as previously published,[12] and as described in Supplemental Methods along with details of variant filtration.[38-42] We selected gene variants that were called in ≥ 1 strain, but not all strains within each patient. We focused on non-synonymous amino acid substitutions, disrupted start or stop codons, and frameshift insertions or deletions. Aneuploidy, gene deletions/duplications and LOH events were analyzed using Ymap [43] and reference genome SC5314 (CGD: A21-s02-m09-r10). We used the allelic ratio (0 or 1 for homozygous regions and 0.5 for heterozygous regions in a diploid genome) to determine whether a region that had SNPs in the parent/reference strain had undergone LOH to become homozygous. Allelic ratio was calculated for each coordinate by dividing the number of reads with the more abundant base call by the total number of reads at each coordinate (resulting in values ranging from 0.5 to 1.0). We selected internal strains for each patient to create a haplotype map and investigate within-patient LOH events.

***In vitro* phenotypic assays.** Growth rate, filamentation, antifungal susceptibility, micafungin tolerance, dot blot and biofilm assays were performed using well-established protocols, as described in detail in Supplemental Methods.[15,16,44]

Chromosome copy numbers.[14] Chr5 (G strains) and Chr7 (MN strains) copy numbers were determined by quantitative real-time PCR (qPCR) as previously described using primer pairs spanning different regions of the chromosomes [Supplemental Table 4]. qPCR of Chr1 and Chr4 served as copy number controls.[14]

Gene expression analysis by qRT-PCR was performed as previously described,[14] using SYBR Green qPCR Master Mix and 1:10 diluted cDNA. Target gene expression was calculated using the ΔΔCT method, with normalization to housekeeping genes *ACT1* and 18S rDNA.

***NRG1* over-expression strain.** The *NRG1* promoter was replaced with the constitutively expressed *TDH3* promoter from plasmid pCJN542 (provided by Aaron Mitchell).[45] Euploid strains M2 and N1 were transformed using PCR products from template plasmid pCJN542 and primers NRG1-OE-F and NRG1-OE-R. Overexpression strains were selected on YPD+clonNAT (YPD, 200 µg/mL nourseothricin sulfate) plates. Integration of constructs was verified by PCR.

Barcoded strains were constructed as previously described.[14] Plasmids RB793 (Addgene #199121) and RB794 (Addgene #199122) containing barcodes were digested with NgoMIV and transformed into target strains. Transformants were selected on YPD+200 µg/mL nourseothricin and confirmed for integration at the *NEUT5L* locus by PCR using primers listed in Supplemental Table 4. *In vitro* growth rates and biofilm formation for barcoded and parent strains were assessed to screen for polar effects.

***In vitro* competitive growth.** Barcoded strains were grown overnight in liquid YPD at 30ºC, washed with PBS and diluted to 10^4/mL in YPD. Cells (1:1 strain mixture, $1x10^4$ CFU/mL each) were incubated at 39ºC with shaking at 200rpm. Micafungin (0.125 µg/mL) or H_2O_2 (1 mM) were added on d0, 3 and 6. On d0, 3, 6 and 9, 200µL aliquots were removed and DNA was extracted for bar code sequencing.

GI colonization in mice. We used 8 mice (equal numbers of male and female mice, 4-6 weeks old, 20-25 g, ICR CD1, Envigo) at each time point. The GI model was performed as previously described.[14] Four days before infection, drinking water was supplemented with 1.5mg/mL ampicillin, 2mg/mL streptomycin and 2.5% glucose. Two barcoded strains were mixed 1:1 and mice were gavaged with $1X10^8$ CFU of each strain. Fecal pellets were collected on d1, 3, and 7, and homogenized in sterile PBS. On d7, stomach, ileum and colon were resected and homogenized in PBS. For *C. albicans* enumeration, fecal samples and organ homogenates were plated on SDA plates with 200µg/mL each of ampicillin, streptomycin, chloramphenicol, kanamycin and nourseothricin. Fecal samples and GI organ homogenates were processed for DNA extraction.[14]

DC model. We inoculated 6 male or female mice per time point for co-infections and 8 mice per strain per time point for mono-infections via lateral tail vein; inocula were $5x10^5$ cells per barcoded strain (co-infection) or $1x10^6$ cells (mono-infection). In co-infections, an additional 6 mice were treated with a single dose of micafungin (8.3 mg/kg/mouse intraperitoneal, 30 minutes post-infection) and sacrificed at 24h. Kidneys from co-infected mice were homogenized for DNA extraction and barcode sequencing on d1, 3 and 7 post-infection.[14] Kidneys from mono-infected mice were processed for histopathologic studies or homogenized and enumerated on SDA for tissue burden determination.

Barcode sequencing. DNA from *in vitro* experiments, fecal samples and organ homogenates was extracted (Zymobiomics DNA Miniprep kit; Zymo Research). Undiluted DNA (1 to 3 µL) from stool or organs was used per 50 µL PCR, as previously described[14] [Supplemental Table 4]. PCR conditions were: 98°C for 30s, 98°C for 10s, 60°C for 30s, 72°C for 30s; steps 2 to 4 repeated for 34 cycles; and 72°C for 5 min. PCR products were gel purified (Wizard SV gel and PCR clean-up system, Promega). ExpressPlex library preparation and sequencing was done by SeqWell (MA, USA). Individual strains were identified by 0-bp unique barcode using CLC

Genomic workbench v.22.0.1. BC1/BC2 ratio was calculated and normalized by the initial inoculum. Fraction (in percent) of BC2 was calculated as: 1/(Ratio+1)X100%.

Populations in longitudinal BC bottles. Percentages of Tri7 and euploid strains were determined by screening 96 strains from a given BC for attenuated biofilm formation as a marker for Tri7 (defined as mean biofilm OD_{590} of 3 independent experiments <30% of mean biofilm formed by euploid strain M2). Ploidy was confirmed by qPCR for ≥ 10 strains from each of d0 and d13 BCs.

Spiking of sterile BC bottles. As previously described, 50 µL of a single colony of Tri7 M1 suspended in saline was inoculated into a sterile BC bottle (Fisher Scientific BD BACTEC Plus Aerobic medium BD442023) that contained 5 mL blood from a healthy volunteer (~1 CFU/mL), and incubated at 37°C with shaking at 225 rpm until turbidity was evident.[12] Ten microliters were streaked on an SDA plate, and incubated at 30°C for 48h. Single strains were isolated from 10 randomly chosen individual colonies for DNA extraction and Illumina sequencing.

Statistical analyses. Statistical analyses were performed using GraphPad Prism version 9.1.2. Data are presented as means and standard error for symmetric data and as medians and interquartile ranges (IQR) for asymmetric data. CFU/g of stool samples or tissues were log-transformed prior to analysis. Student t-test or Mann-Whitney U tests were used for comparisons of 2 groups, and one-way ANOVA or Kruskal-Wallis for comparisons of >2 groups. For all analyses, $p < 0.05$ (two-tailed) was considered significant.

DATA AVAILABILITY. Datasets for this study are available in data files submitted with this article. Data are presented in the article, Supplementary Material and Supplemental Data Files. WGS data have been deposited in the NCBI database under accession number PRJNA1118730.

Table 1. Clinical characteristics, treatment and outcomes of patients with *Candida albicans* bloodstream infections

Patient	Features of bloodstream infection (BSI) Duration of BSI*	Antifungal minimum inhibitory concentrations (MICs) against index strain	Antifungal treatment and outcome**	Positive blood cultures (BCs) for WGsing and strain nomenclature***
MN	Endovascular infection Duration of BSI: 13 days	AmB: 0.5 µg/mL CSP: 0.125 µg/mL FLU: 0.125 µg/mL POS: 0.015 µg/mL VOR: 0.015 µg/mL	CSP: days 2-6 CSP+FLU: days 6-7 AmB: days 8-14 FLU: day 15 - plan for lifelong Alive, on chronic suppressive FLU	Baseline (D0): M1 to M5 D13 BC: N1 to N5
AB	Central line associated BSI Duration of BSI: 3 days	AmB: 0.5 µg/mL CSP: 0.125 µg/mL FLU: 0.06 µg/mL POS: 0.015 µg/mL VOR: 0.015 µg/mL	CSP: days 3-4 FLU: days 5-7 Alive	Baseline (D0): A1 to A5 D3 BC: B1 to B5
G	Intra-abdominal and ocular candidiasis Duration of BSI: 1 day	AmB: 0.5 µg/mL CSP: 0.5 µg/mL FLU: 0.06 µg/mL POS: 0.015 µg/mL VOR: 0.015 µg/mL	CSP: day 4 FLU: days 4-15 Alive	Baseline (D0): G1-G10
QR	Endovascular infection Duration of BSI: 12 days	AmB: 0.5 µg/mL CSP: 0.35 µg/mL FLU: 0.06 µg/mL POS: 0.015 µg/mL VOR: 0.015 µg/mL	CSP: days 1-2, days 21-40 FLU: days 3-4, D40-death CAP+FLU: days 5-20 No BSI recurrence after day 12 Died from liver failure	Baseline (D0): Q1 to Q5 D12 BC: R1 to R5

*Duration of BSI is dated from baseline positive blood culture on day 0. Therefore, 2 days would signify a positive blood culture collected 48-72 hours after the baseline positive blood culture was collected. **Days of antifungal treatment are dated from positive baseline blood culture on day 0. ***In 3 patients (MN, AB, QR), baseline positive (i.e., time of diagnosis) and last positive blood cultures collected after the institution of antifungal treatment were included in whole genome sequencing studies. For 1 patient (G), only the baseline blood culture was included.

WGSing: whole genome sequencing; D: day(s); AmB: amphotericin B; CSP: caspofungin; FLU: fluconazole; POS: posaconazole; VOR: voriconazole

Table 2. **Within-patient genetic variations among *Candida albicans* strains from blood cultures.**

Patient	BC bottle (time points)	Strains	SNPs					INDELs		Aneuploidy	LOH
			Total SNPs	Syn		Non-Syn					
				Het	Hom	Het	Hom	Het	Hom		
AB	Day 0	A1	7	3	1	2	1	0	0	-	
		A2	4	2	0	1	1	0	0	-	-
		A3	3	0	1	1	1	0	0	-	-
		A4	1	0	1	0	0	0	0	-	-
		A5	0	0	0	0	0	0	0	-	-
	Day 3	B1	3	2	0	0	1	0	0	-	-
		B2	2	0	1	0	1	0	0	-	-
		B3	4	2	0	1	1	0	0	-	-
		B4	0	0	0	0	0	0	0	-	-
		B5	3	1	1	0	1	0	0	-	-
G	Day 0	G1	42	5	9	10	18	7	1	trisomy Chr 5	-
		G2	19	4	3	7	5	2	1	-	-
		G3	13	3	2	4	4	3	0	-	-
		G4	15	3	3	7	2	3	0	-	-
		G5	7	1	2	2	2	1	1	-	-
		G6	28	3	6	7	12	1	0	-	-
		G7	20	3	4	7	6	6	2	-	-
		G8	30	3	5	9	13	5	1	-	-
		G9	11	1	3	3	4	1	2	-	-
		G10	15	4	1	7	3	5	0	-	-
MN	Day 0	M1	18	5	2	7	4	2	0	trisomy Chr 7	-
		M2	23	5	2	13	3	3	0	-	-
		M3	30	6	9	9	6	1	0	trisomy Chr 7	-
		M4	3	0	0	3	0	1	0	trisomy Chr 7	-

		M5	19	4	6	6	3	0	0	trisomy Chr 7	-
	Day 14	N1	13	3	2	3	5	0	0	-	-
		N2	36	6	6	18	6	7	2	-	-
		N3	3	0	0	3	0	0	0	-	-
		N4	29	4	8	11	6	2	0	-	-
		N5	18	2	2	12	2	4	0	-	-
QR	Day 0	Q1	24	1	5	7	11	4	0	-	Chr 1
		Q2	28	3	5	6	14	5	1	-	Chr 1
		Q3	19	8	2	9	0	4	0	-	
		Q4	23	2	5	5	11	1	0	-	
		Q5	24	2	5	5	12	2	1	-	
	Day 12	R1	10	2	1	5	2	2	0	-	Chr 1
		R2	8	3	0	5	0	1	0	-	Chr 1
		R3	18	1	4	3	10	2	0	-	Chr 1
		R4	12	3	1	5	3	2	3	-	Chr 1
		R5	18	1	4	3	10	1	0	-	Chr 1

SNPs and INDELs reported were defined as variants present in ≥ 1 strain but not all strains from a given patient, compared to reference strain SC5314

BC: blood culture; SNP: single nucleotide polymorphism; indel: insertion-deletion; LOH: loss of heterozygosity; syn: synonymous; non-syn: non-synonymous; het: heterozygous; hom: homozygous; chr: chromosome

1. Sitterlé E, Maufrais C, Sertour N, Palayret M, D'Enfert C, Bougnoux M-E. Within-Host Genomic Diversity of Candida albicans in Healthy Carriers. Scientific Reports 2019;9.
2. Anderson FM, Visser ND, Amses KR, et al. Candida albicans selection for human commensalism results in substantial within-host diversity without decreasing fitness for invasive disease. PLOS Biology 2023;21:e3001822.
3. Gabaldon T, Carrete L. The birth of a deadly yeast: tracing the evolutionary emergence of virulence traits in Candida glabrata. FEMS Yeast Res 2016;16:fov110.
4. Hickman MA, Zeng G, Forche A, et al. The 'obligate diploid' Candida albicans forms mating-competent haploids. Nature 2013;494:55-9.
5. Hirakawa MP, Martinez DA, Sakthikumar S, et al. Genetic and phenotypic intra-species variation in Candida albicans. Genome Research 2015;25:413-25.
6. Carreté L, Ksiezopolska E, Gómez-Molero E, et al. Genome Comparisons of Candida glabrata Serial Clinical Isolates Reveal Patterns of Genetic Variation in Infecting Clonal Populations. Frontiers in Microbiology 2019;10.
7. Munoz JF, Gade L, Chow NA, et al. Genomic insights into multidrug-resistance, mating and virulence in Candida auris and related emerging species. Nat Commun 2018;9:5346.
8. Didelot X, Walker AS, Peto TE, Crook DW, Wilson DJ. Within-host evolution of bacterial pathogens. Nat Rev Microbiol 2016;14:150-62.
9. Moxon ER, Murphy PA. Haemophilus influenzae bacteremia and meningitis resulting from survival of a single organism. Proc Natl Acad Sci U S A 1978;75:1534-6.
10. Rubin LG. Bacterial colonization and infection resulting from multiplication of a single organism. Rev Infect Dis 1987;9:488-93.
11. Young BC, Wu CH, Gordon NC, et al. Severe infections emerge from commensal bacteria by adaptive evolution. Elife 2017;6.
12. Badrane H, Cheng S, Dupont CL, et al. Genotypic diversity and unrecognized antifungal resistance among populations of Candida glabrata from positive blood cultures. Res Sq 2023.
13. Cheng S, Fleres G, Chen L, et al. Within-Host Genotypic and Phenotypic Diversity of Contemporaneous Carbapenem-Resistant Klebsiella pneumoniae from Blood Cultures of Patients with Bacteremia. mBio 2022;13:e0290622.
14. Kakade P, Sircaik S, Maufrais C, Ene IV, Bennett RJ. Aneuploidy and gene dosage regulate filamentation and host colonization by Candida albicans. Proceedings of the National Academy of Sciences 2023;120.
15. Rosenberg A, Ene IV, Bibi M, et al. Antifungal tolerance is a subpopulation effect distinct from resistance and is associated with persistent candidemia. Nat Commun 2018;9:2470.
16. Berman J, Krysan DJ. Drug resistance and tolerance in fungi. Nat Rev Microbiol 2020;18:319-31.
17. Rottmann M, Dieter S, Brunner H, Rupp S. A screen in Saccharomyces cerevisiae identified CaMCM1, an essential gene in Candida albicans crucial for morphogenesis. Mol Microbiol 2003;47:943-59.
18. Anderson MZ, Saha A, Haseeb A, Bennett RJ. A chromosome 4 trisomy contributes to increased fluconazole resistance in a clinical isolate of Candida albicans. Microbiology 2017;163:856-65.
19. Selmecki A, Gerami-Nejad M, Paulson C, Forche A, Berman J. An isochromosome confers drug resistance in vivo by amplification of two genes, ERG11 and TAC1. Molecular Microbiology 2008;68:624-41.
20. Yang F, Todd RT, Selmecki A, Jiang Y-Y, Cao Y-B, Berman J. The fitness costs and benefits of trisomy of each Candida albicans chromosome. Genetics 2021;218.
21. Ene IV, Farrer RA, Hirakawa MP, Agwamba K, Cuomo CA, Bennett RJ. Global analysis of mutations driving microevolution of a heterozygous diploid fungal pathogen. Proceedings of the National Academy of Sciences 2018;115:E8688-E97.
22. Forche A, Cromie G, Gerstein AC, et al. Rapid Phenotypic and Genotypic Diversification After Exposure to the Oral Host Niche in Candida albicans. Genetics 2018;209:725-41.
23. Forche A, Solis NV, Swidergall M, et al. Selection of Candida albicans trisomy during oropharyngeal infection results in a commensal-like phenotype. PLOS Genetics 2019;15:e1008137.
24. Tso GHW, Reales-Calderon JA, Tan ASM, et al. Experimental evolution of a fungal pathogen into a gut symbiont. Science 2018;362:589-95.

25. Knoll MA, Lackner N, Ulmer H, et al. Multiple colony antifungal susceptibility testing detects polyresistance in clinical Candida cultures: a European Confederation of Medical Mycology excellence centers study. Clin Microbiol Infect 2022;28:1288 e1- e7.
26. Gerstein AC, Cleathero LA, Mandegar MA, Otto SP. Haploids adapt faster than diploids across a range of environments. J Evol Biol 2011;24:531-40.
27. Arastehfar A, Daneshnia F, Cabrera N, et al. Macrophage internalization creates a multidrug-tolerant fungal persister reservoir and facilitates the emergence of drug resistance. Nat Commun 2023;14:1183.
28. Shields RK, Nguyen MH, Potoski BA, et al. Doripenem MICs and ompK36 porin genotypes of sequence type 258, KPC-producing Klebsiella pneumoniae may predict responses to carbapenem-colistin combination therapy among patients with bacteremia. Antimicrob Agents Chemother 2015;59:1797-801.
29. Yang F, Berman J. Beyond resistance: antifungal heteroresistance and antifungal tolerance in fungal pathogens. Current Opinion in Microbiology 2024;78:102439.
30. Suwunnakorn S, Wakabayashi H, Rustchenko E. Chromosome 5 of Human Pathogen Candida albicans Carries Multiple Genes for Negative Control of Caspofungin and Anidulafungin Susceptibility. Antimicrobial Agents and Chemotherapy 2016;60:7457-67.
31. Yang F, Gritsenko V, Slor Futterman Y, et al. Tunicamycin Potentiates Antifungal Drug Tolerance via Aneuploidy in Candida albicans. mBio 2021;12.
32. Yang F, Teoh F, Tan ASM, Cao Y, Pavelka N, Berman J. Aneuploidy Enables Cross-Adaptation to Unrelated Drugs. Molecular Biology and Evolution 2019;36:1768-82.
33. Yang F, Zhang L, Wakabayashi H, et al. Tolerance to Caspofungin in Candida albicans Is Associated with at Least Three Distinctive Mechanisms That Govern Expression of FKS Genes and Cell Wall Remodeling. Antimicrobial Agents and Chemotherapy 2017;61:AAC.00071-17.
34. Saville SP, Lazzell AL, Monteagudo C, Lopez-Ribot JL. EngineeredControl of Cell Morphology In Vivo Reveals Distinct Roles for Yeast andFilamentous Forms of Candida albicans duringInfection. Eukaryotic Cell 2003;2:1053-60.
35. Mao Y, Solis NV, Filler SG, Mitchell AP. Functional Dichotomy for a Hyphal Repressor in Candida albicans. mBio 2023;14:e0013423.
36. Wakade RS, Wellington M, Krysan DJ. The role of the C. albicans transcriptional repressor NRG1 during filamentation and disseminated candidiasis is strain dependent. mSphere 2024;9:e0078523.
37. Uppuluri P, Pierce CG, Thomas DP, Bubeck SS, Saville SP, Lopez-Ribot JL. The Transcriptional Regulator Nrg1p Controls Candida albicans Biofilm Formation and Dispersion. Eukaryotic Cell 2010;9:1531-7.
38. McKenna A, Hanna M, Banks E, et al. The Genome Analysis Toolkit: A MapReduce framework for analyzing next-generation DNA sequencing data. Genome Research 2010;20:1297-303.
39. Cingolani P, Platts A, Wang LL, et al. A program for annotating and predicting the effects of single nucleotide polymorphisms, SnpEff. Fly 2012;6:80-92.
40. Danecek P, Bonfield JK, Liddle J, et al. Twelve years of SAMtools and BCFtools. GigaScience 2021;10.
41. Kozlov AM, Darriba D, Flouri T, Morel B, Stamatakis A. RAxML-NG: a fast, scalable and user-friendly tool for maximum likelihood phylogenetic inference. Bioinformatics 2019;35:4453-5.
42. Letunic I, Bork P. Interactive Tree Of Life (iTOL) v5: an online tool for phylogenetic tree display and annotation. Nucleic Acids Research 2021;49:W293-W6.
43. Abbey DA, Funt J, Lurie-Weinberger MN, et al. YMAP: a pipeline for visualization of copy number variation and loss of heterozygosity in eukaryotic pathogens. Genome Medicine 2014;6.
44. Institute CaLS. Reference Method for Broth Dilution Antifungal Susceptibility Testing of Yeasts. 4th ed. CLSI standard M27. Wayne, PA: Clinical and Laboratory Standards Institute; 2017.
45. Nobile CJ, Solis N, Myers CL, et al. Candida albicans transcription factor Rim101 mediates pathogenic interactions through cell wall functions. Cell Microbiol 2008;10:2180-96.

Figure 1. **Core genome single nucleotide polymorphism (SNP) phylogenetic tree of *Candida albicans* strains from patients with bloodstream infections.** Ten strains from each of 4 patients (AB (magenta), G (green), MN (blue) and QR (yellow)) underwent whole genome sequencing. The phylogenomic tree was built using RaxML under the general time-reversible model with 1,000-bootstrap replicates. Within-patient strains had the following ranges of SNP differences: patient AB (range, 0-7); patient G (range, 7-42); patient MN (range, 3-36); patient QR (range, 8-28). Nodes grouping by clade and patient had 100% bootstrap support values.

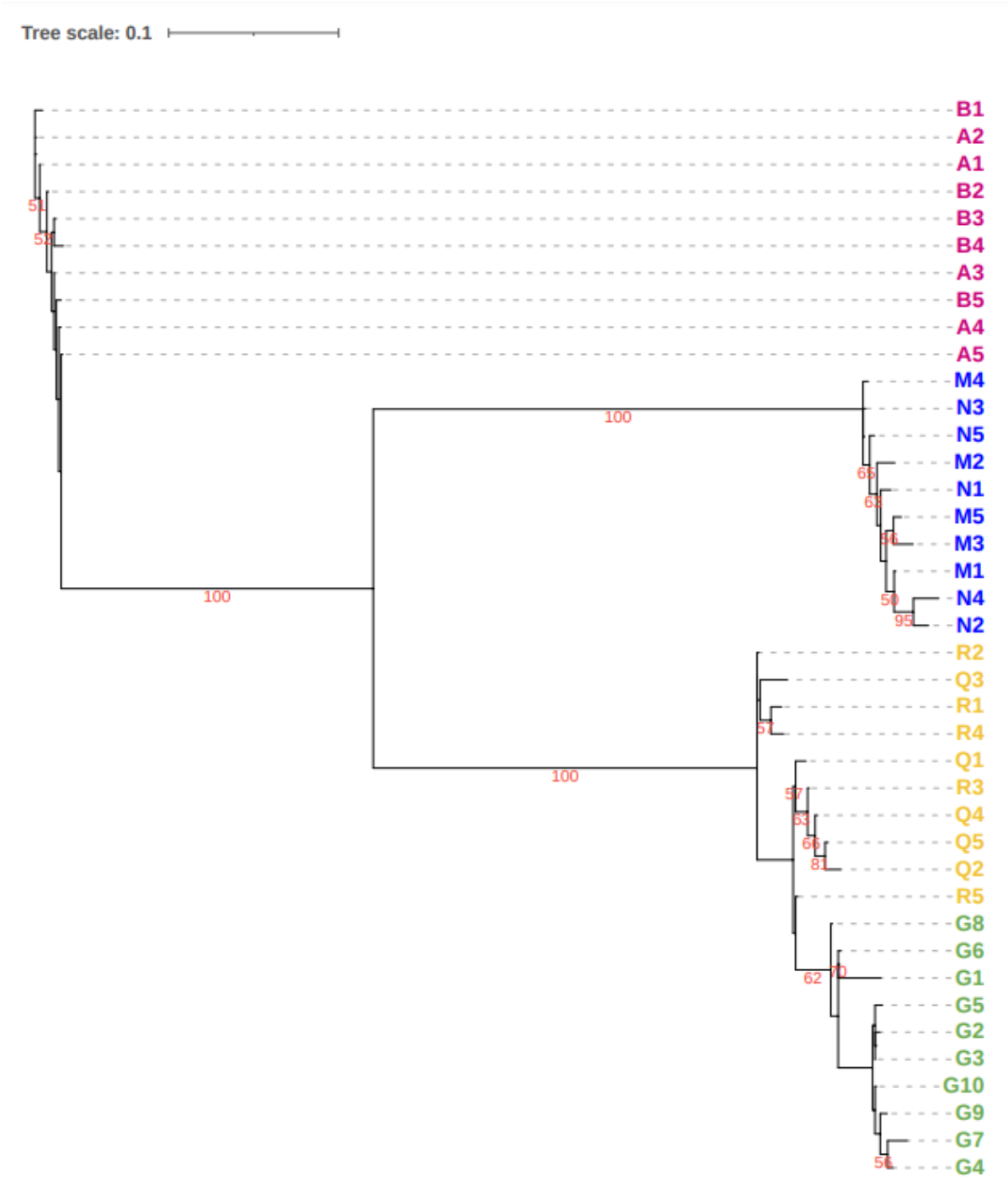

Figure 2. Copy number variations (CNVs), single nucleotide polymorphism (SNP) density and loss of heterozygosity (LOH) in *Candida albicans* strains from patients with bloodstream infections. Strains from patients G, MN and QR are shown in Figures A through C, respectively. Chromosomes are arranged along the horizontal (x) axis. The vertical (y) axis represents sequence read depth, scaled to actual copy number. CNVs are presented as black lines drawn upwards or downwards from the mid-line of the chromosome. Regions with CNV are highlighted in green. Regions of SNP density are presented as shades of grey, and homozygous regions are white. Regions of LOH are red. Black circles along the bottom of chromosomes represent major repeat sequences (MRSs). **A.** Strain G1 differed from other G strains by having an extra copy of whole Chr5 (i.e., trisomy 5), as evident by a block of black lines extending upward from the mid-line (green highlight). Strains did not differ by SNP density or LOH. **B.** Strains M1, M3, M4 and M5 differed from other MN strains by having an extra copy of whole Chr7 (i.e., trisomy 7). All MN strains had an extra copy of a small region adjacent to the second MRS of Chr7 (green highlight). Strains did not differ by SNP density or LOH. **C.** Strains Q1, Q2 and R1-R5 had a region of LOH (red highlight) in a segment at the end of the left arm of chromosome 1, which was not apparent in strains Q3-Q5. As indicated by grey highlight, the latter strains did not have gaps in SNP density in the region of LOH. A small potential region of LOH was also present uniquely in strains R1-R5, demarcated by a single red line near the middle of the left arm of Chr7; the size of this region was at or very near the resolution limit for YMAP analysis (4.5 Kb). QR strains did not differ by CNV or ploidy. The only differences among strains in SNP density was in the region of LOH.

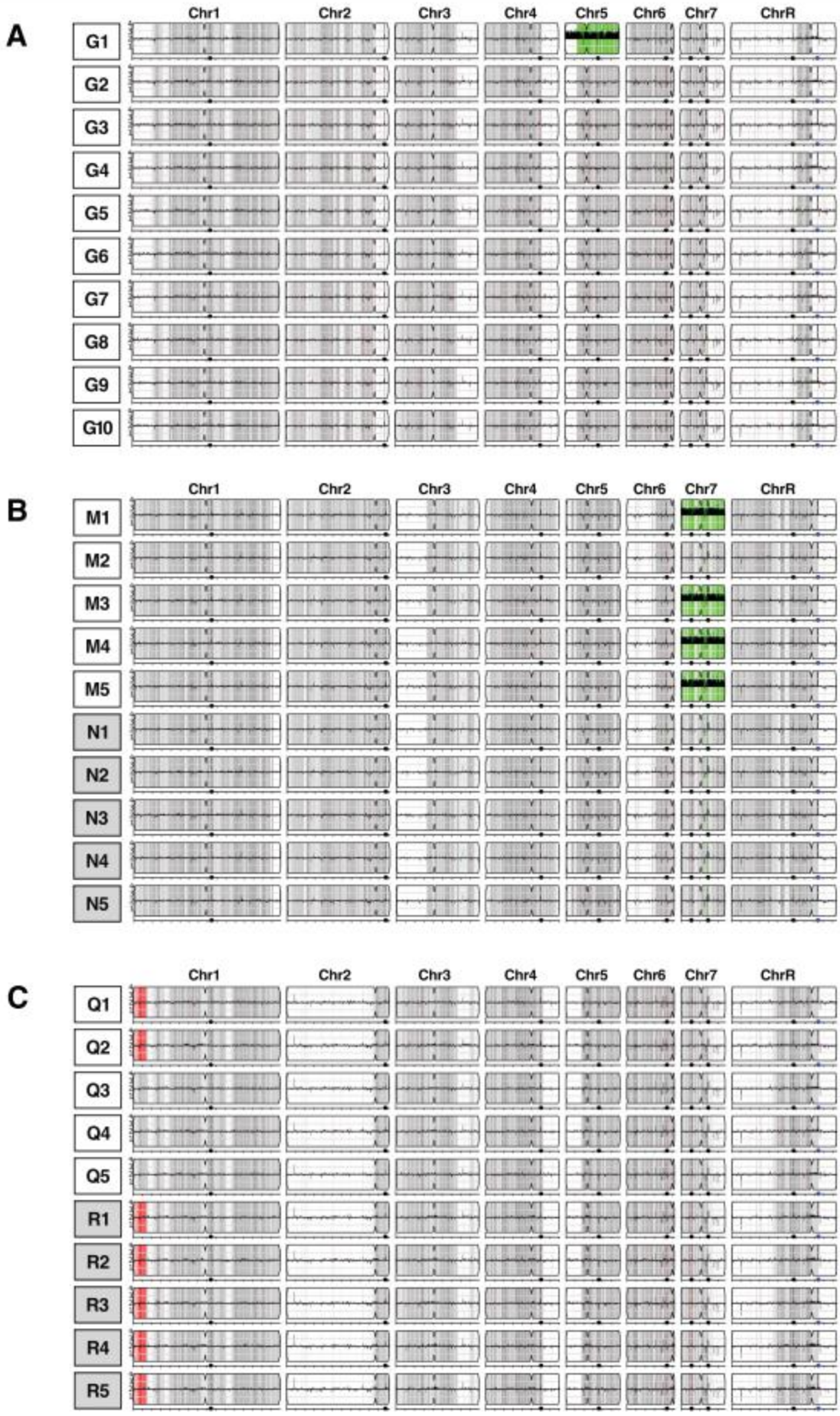
A
Chr1
Chr2
Chr3
Chr4
Chr5
Chr6
Chr7
ChrR
G1
G2
G3
G4
G5
G6
G7
G8
G9
G10
B
M1
M2
M3
M4
M5
N1
N2
N3
N4
N5
C
Q1
Q2
Q3
Q4
Q5
R1
R2
R3
R4
R5

Figure 3. Hyphal formation by MN strains on solid agar. Strains were photographed after incubation on RPMI 1640 with 2% glucose medium at 30°C for 5 days. Euploid strains (M2, N1, N2, N3, N4 and N5) formed extensive hyphae, whereas trisomy 7 strains M1, M3, M4 and M5 did not.

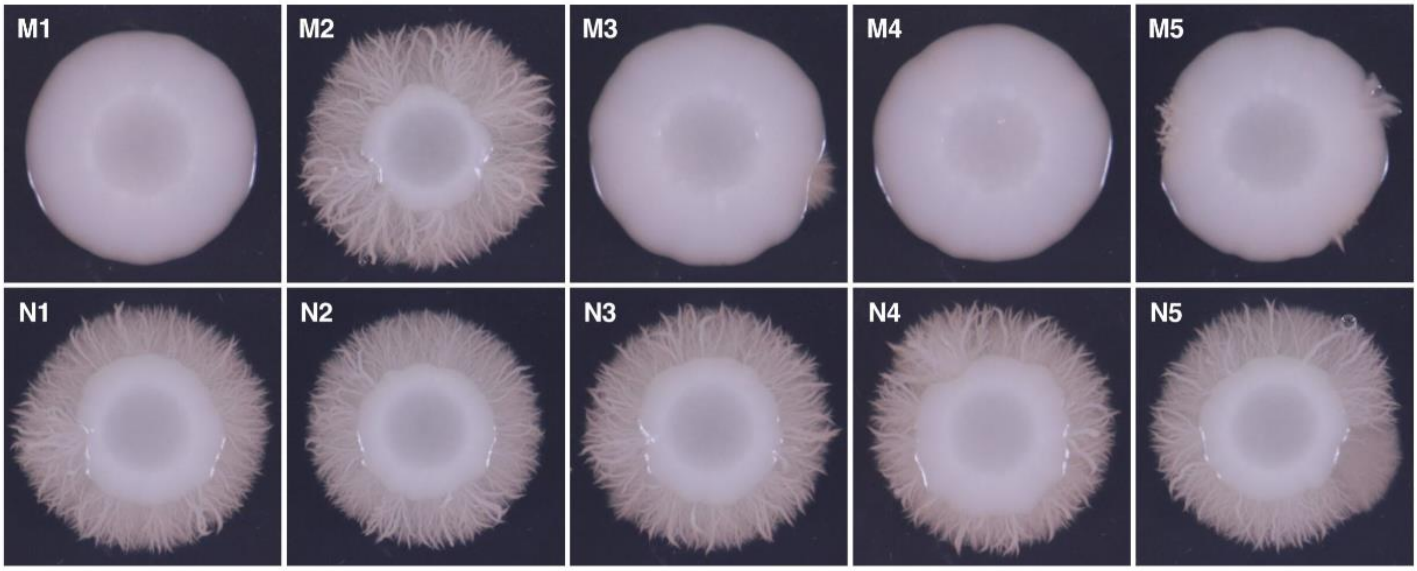

Figure 4. Timeline of *Candida albicans*-positive blood cultures (BCs) and antifungal treatment for patient MN. The baseline positive BC (i.e., BC at time of initial diagnosis) was collected on day 0. Antifungal treatment was initiated with caspofungin on day 2, after baseline BC results were reported by the clinical microbiology lab. Subsequent BCs that were positive for *C. albicans* were collected on days 3, 5, 10 and 13. The percentage of strains from each positive BC that had trisomy of Chr7 (Tri7) is shown at the bottom of the figure and represented as black in the bar graph. The percentage of strains that were euploid for Chr7 are represented by white in the bar graph. CSP, caspofungin; FLU, fluconazole; AmB, amphotericin B

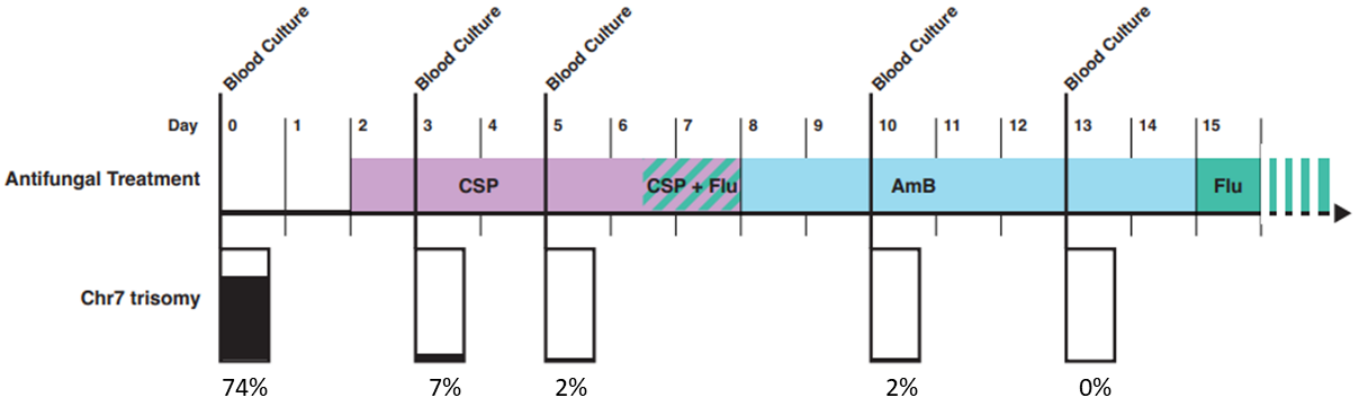

Figure 5. Susceptibility of MN strains to cell wall-active agents. Serial 10-fold dilutions starting at $1x10^6$ CFU/mL of trisomy7 and euploid strains were spotted at exponential growth onto Sabouraud dextrose agar (SDA, control) and SDA containing Congo red (200µg/mL), sodium dodecyl sulfate (SDS, 0.04%) or micafungin (0.03 µg/mL). Plates were incubated at 39°C or 30°C for 3d. Images are shown for representative trisomy7 (M1, M3) and euploid (M2, N1) strains on d3 at 39°C. Phenotypes were similar at 30°C.

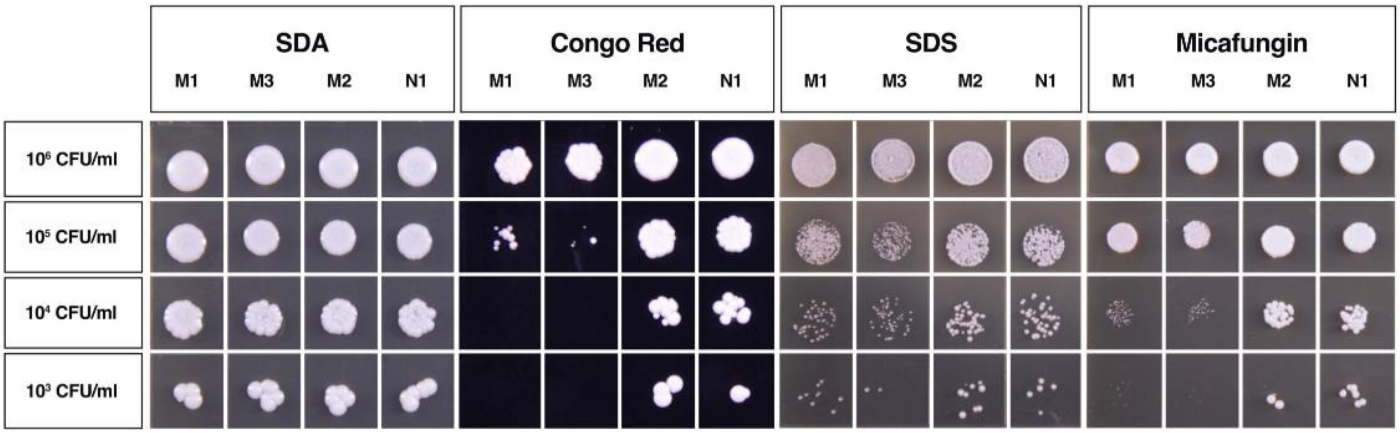

Figure 6. Evaluation of micafungin tolerance using (A) disk diffusion assay (fraction of growth, FoG) and (B) broth microdilution assay (supra-MIC growth, SMG). A. A filter disc inoculated with 5 µg of micafungin was placed in the middle of a casitone agar place saturated with *C. albicans* strains. Tolerance was determined at 48h growth at 35°C. The fraction of growth (FoG) was defined as growth within the region of inhibition relative to the maximum growth. FoG was calculated by diskImageR and image J at 80%, 50% and 20% relative inhibition (referred to as FOG_{80}, FOG_{50} and FOG_{20}, respectively). Data shown are mean ± standard error of means of FoG values for Tri7 and euploid strains. *P*-values were determined by student's t test with Welsh correction (* denotes $p < 0.05$ and ** $p < 0.01$). **B.** SMG was determined using a broth microdilution assay and defined as the proportion of average of growth at 48h in wells with drug concentration above the MIC relative to the growth of no drug control wells. SMG data (OD_{600} at 48h) are presented as mean ± standard error of euploid and Tri7 strains on a bar graph (top), and as a heat map (bottom). Heat map scale is shown on the bottom right.

9

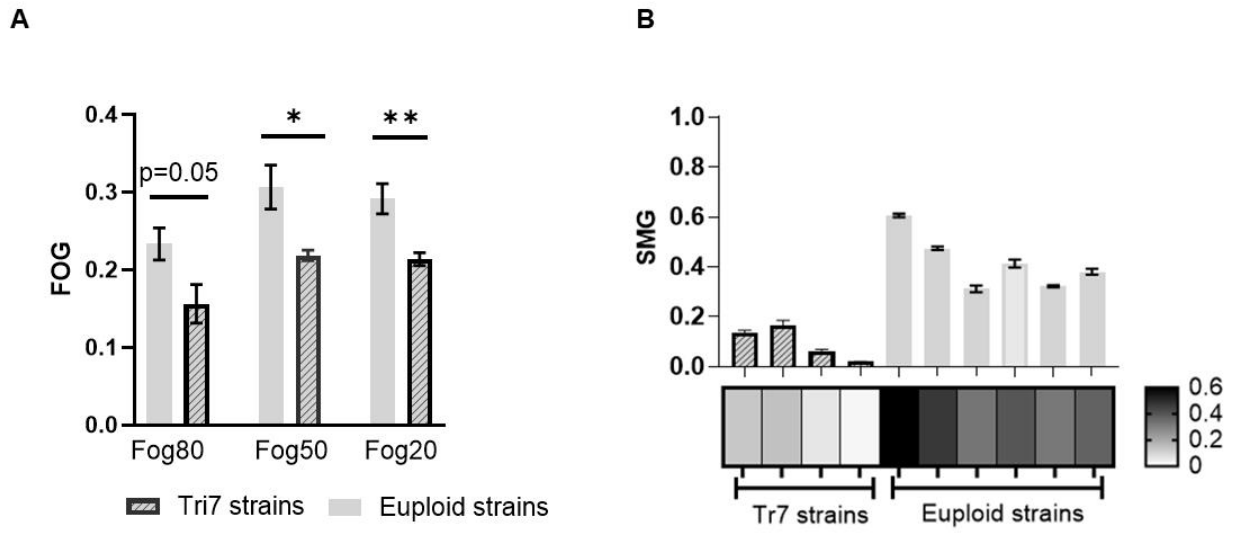

Figure 7. Biofilm formation by MN strains. Biofilm formation by MN strains at 37°C in RPMI1640 medium supplemented with 2% (w/v) glucose was measured by a 0.1% aqueous crystal violet assay in flat bottom wells as optical density at 590 nm (OD_{590}). Data are presented as mean ± SEM of ratio of OD_{590} for a given strain relative to that of euploid strain M2 (3 independent experiments). Tri7 (M1, M3, M4 and M5) and euploid (M2, N1-N5) strains are represented by striped and solid grey bar graphs, respectively. Tri7 strains consistently produced < 30% of biofilm produced by euploid strains (mean ± SEM ratio: 0.17±0.01 *vs*. 0.99±0.04, respectively; ****p<0.0001, Mann-Whitney test). Tri7 strains did not differ significantly from one another in biofilm formation, nor did euploid strains significantly differ among themselves.

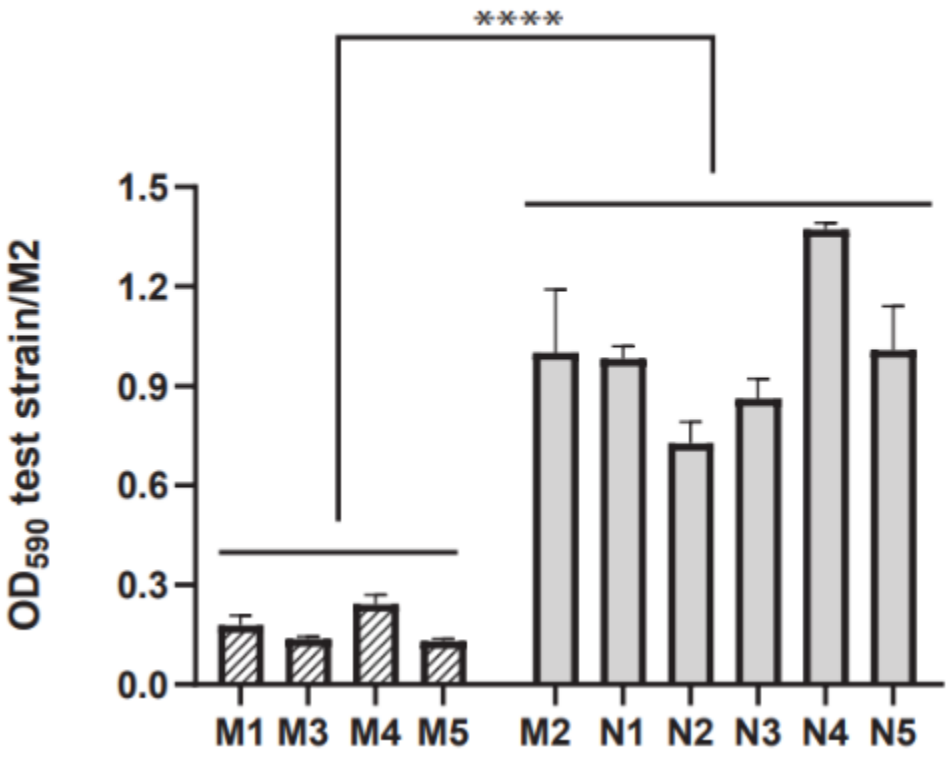

Figure 8. Competitive fitness of trisomy 7 strain M1 and euploid strain M2. Barcoded strains M1 and M2 were mixed 1:1 in all experiments; input ratios were confirmed by colony forming unit determinations. At given timepoints, competitive indices (fraction of total population) of M1 and M2 were determined by barcode sequencing. Data are presented as mean ± SEM competitive indices for each strain from 3 independent experiments. * $p<0.05$, ** $p<0.01$, *** $p<0.001$, **** $p<0.0001$ **A. *In vitro***. Barcoded M1 and M2 were co-cultured in yeast peptone dextrose (YPD) medium at 39°C with or without H_2O_2 (1 mM) or micafungin (0.125 µg/mL) for 3, 6 and 9d. Strains did not differ in fitness in YPD alone or in presence of H_2O_2. M1 was significantly more fit than M2 at each time point in presence of micafungin ($p< 0.0001$; unpaired student's t test). **B. *Ex vivo.*** Strains were co-incubated in human blood at 37°C. Fractions of each strain out of the total population were assessed at d1, d3 and d7. Strain M1 was significantly more fit than M2 at each time point. *P*-values were calculated using one-way ANOVA with Dunnett's multiple comparisons against inoculum fraction. **C, D. Mouse model of gastrointestinal (GI) colonization**. Mice were co-infected via gavage with barcoded M1 and M2 ($1x10^8$ CFU of each strain per mouse). Stool samples were obtained on d1, d3 and d7 after inoculation (2C). On d7, mice were sacrificed, and stomach, ileum and colon were obtained and homogenized for DNA extraction for barcode sequencing (2D). M1 was significantly more fit than M2 within stool at all time points, and more fit than M2 within ileum and colon. Strains did not differ in fitness within stomachs. **E. Mouse model of disseminated candidiasis (DC).** Mice were co-infected via lateral tail vein with barcoded strains M1 and M2 ($5x10^5$ CFU of each strain per mouse). Kidneys were obtained and homogenized for DNA extraction for barcode sequencing on d1, d3 and d7. A group of co-infected mice were treated with a single dose of micafungin (8.3 mg/kg/mouse intraperitoneal, 30 minutes post-infection), and kidneys were obtained for barcode sequencing 24h following treatment. *P*-values for C-E were determined using one-way ANOVA test with Dunn's multiple comparison against inoculum fraction. Tri7 M1 strain was more fit than M2 in the GI and DC models. M2 was significantly more fit within kidneys of mice treated with micafungin than it was within kidneys of untreated mice.

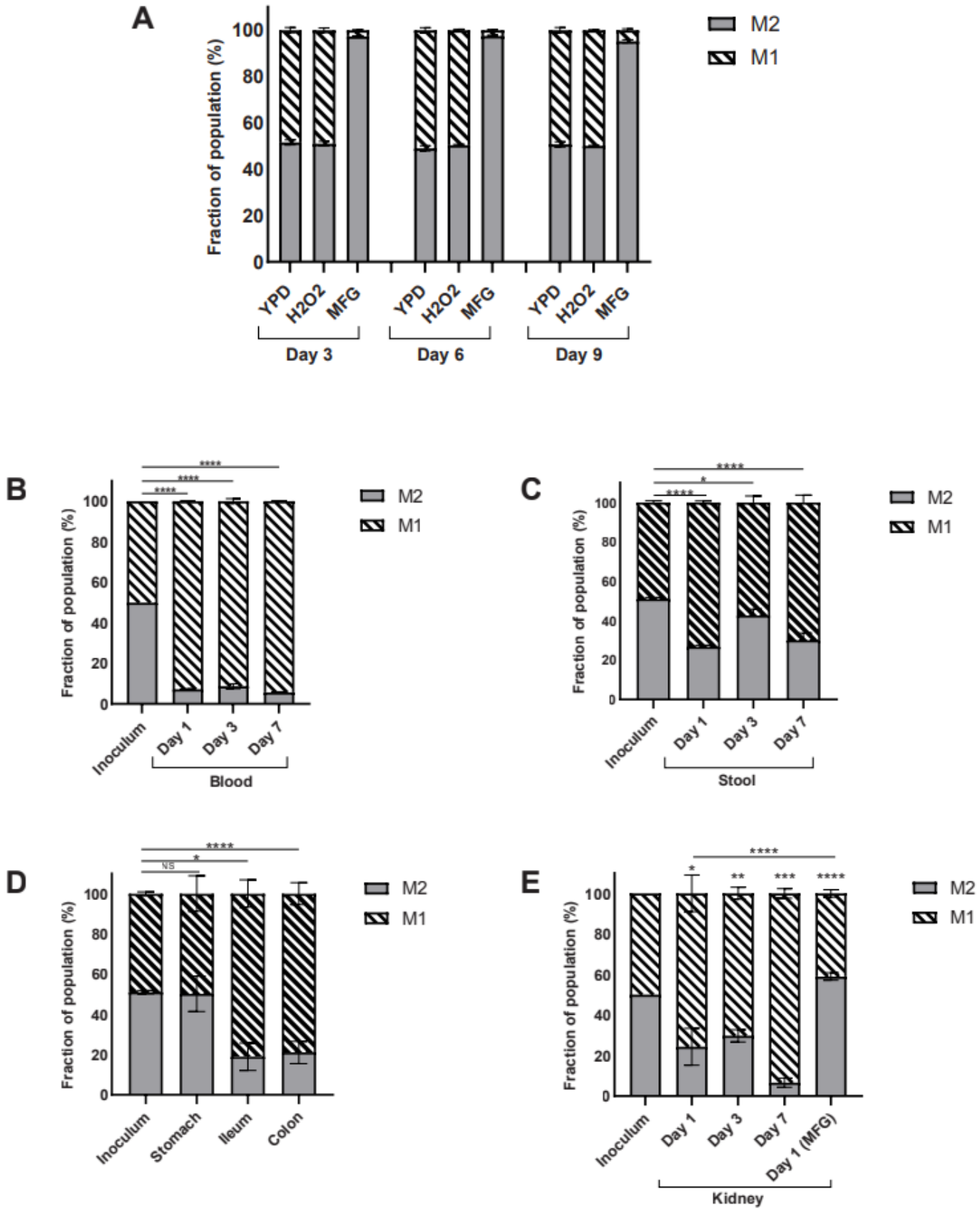
A
Fraction of population (%)
100
80
60
40
20
0
M2
M1
YPD
H2O2
MFG
Day 3
Day 6
Day 9
B
****
****
****
Inoculum
Day 1
Day 3
Day 7
Blood
C
****
*
****
Stool
D
****
*
NS
Stomach
Ileum
Colon
E
*
**
***
****
Day 1 (MFG)
Kidney
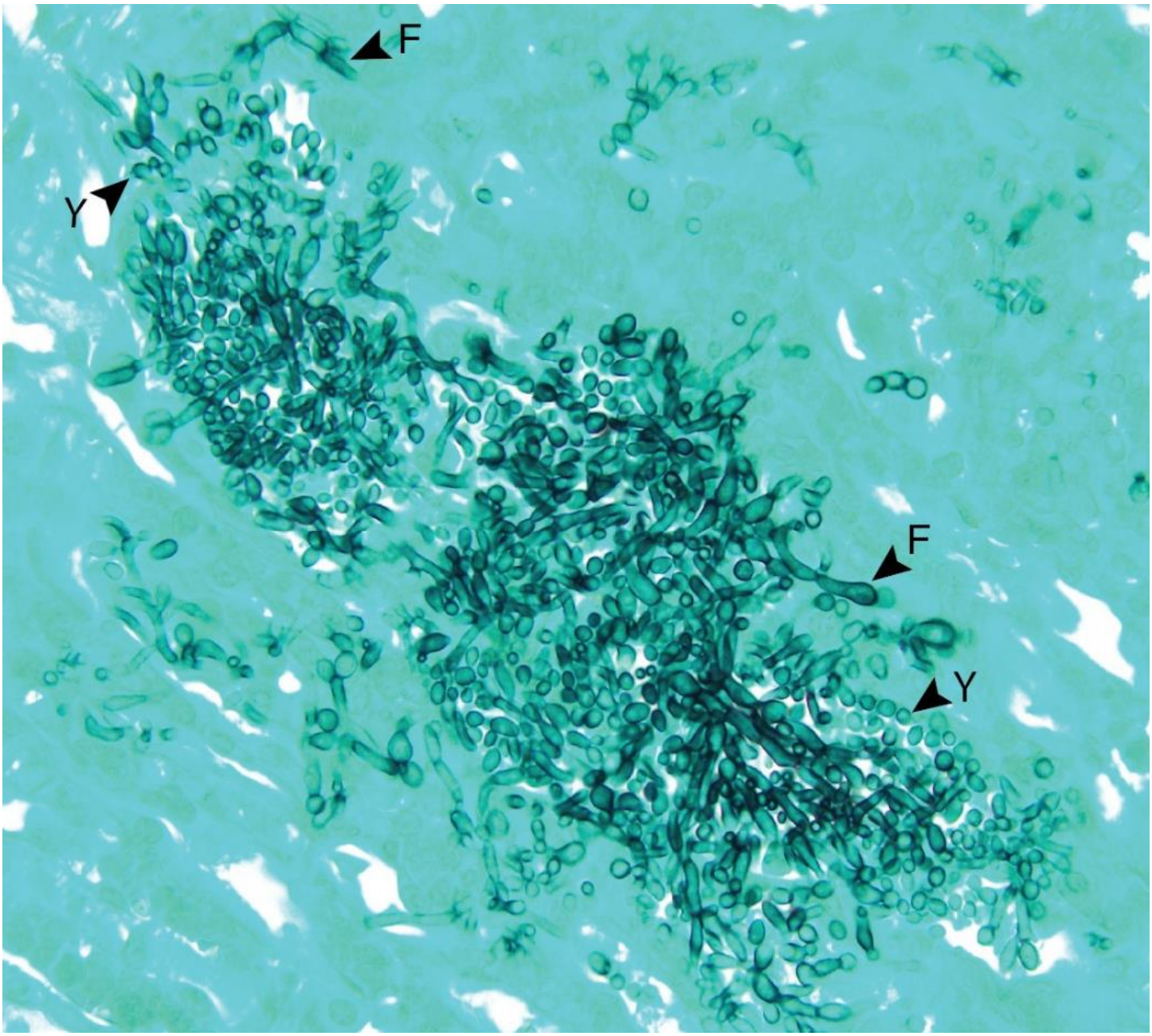
Figure 9. Morphology of strain M1 within mouse kidneys. Kidney sections from mice infected intravenously with barcoded strains M1 or M2 alone were stained with Grocott Methenamine Silver (GMS). Strain M1 is shown growing in filamentous morphologies (denoted by arrowheads labeled with “F”) interspersed with multiple yeasts (arrowhead labeled with “Y”) (image at 400x) within kidneys on d3. Filamentous morphologies included both hyphae and pseudohyphae. M1 morphologies on d1 were similar to those on d3, and they did not differ on either day from M2 morphologies (not shown).